Annals of Botany **XX**: 1–10, 2019
doi: 10.1093/aob/mcz076, available online at www.academic.oup.com/aob

ANNALS OF BOTANY
Founded 1887

The functional implications of tracheary connections across growth rings in four northern hardwood trees

Jay W. Wason[1,2,*], Craig R. Brodersen[2] and Brett A. Huggett[3]

[1]School of Forest Resources, University of Maine, Orono, ME, USA, [2]School of Forestry and Environmental Studies, Yale University, New Haven, CT, USA and [3]Department of Biology, Bates College, Lewiston, ME, USA
**For correspondence. E-mail jay.wason@maine.edu*

Received: 4 January 2019 Returned for revision: 18 March 2019 Editorial decision: 30 April 2019 Accepted: 2 May 2019

• **Background and aims** Deciduous angiosperm trees transport xylem sap through trunks and branches in vessels within annual growth rings. Utilizing previous growth rings for sap transport could increase vessel network size and redundancy but may expose new xylem to residual air embolisms in the network. Despite the important role of vessel networks in sap transport and drought resistance, our understanding of cross-ring connections within and between species is limited.
• **Methods** We studied cross-ring connections in four temperate deciduous trees using dye staining and X-ray microcomputed tomography (microCT) to detect xylem connectivity across growth rings and quantify their impact on hydraulic conductivity.
• **Key results** *Acer rubrum* and *Fraxinus americana* had cross-ring connections visible in microCT but only *A. rubrum* used previous growth rings for axial sap flow. *Fagus grandifolia* and *Quercus rubra*, however, did not have cross-ring connections. Accounting for the number of growth rings that function for axial transport improved hydraulic conductivity estimates.
• **Conclusions** These data suggest that the presence of cross-ring connections may help explain aspects of whole-tree xylem sap transport and should be considered for plant hydraulics measurements in these species and others with similar anatomy.

Key words: *Acer rubrum*, connectivity, diffuse porous, earlywood, *Fagus grandifolia*, *Fraxinus americana*, growth rings, hydraulics, latewood, *Quercus rubra*, ring porous, xylem.

INTRODUCTION

Deciduous angiosperm trees transport xylem sap through the trunk and branches in networks of conduits formed in annual growth rings. Within a growth ring, most axial xylem sap transport occurs in vessels because of their large diameter, and therefore lower resistance, relative to fibres and tracheids. Xylem within the trunk is often divided into two categories: the older, non-functional heartwood and the younger, functional sapwood. Sapwood is typically composed of several annual growth rings, with the majority of xylem sap flowing axially through the current-year xylem (Ellmore and Ewers, 1986; Melcher *et al.*, 2003), but the contribution of previously formed growth rings is variable among species and wood types (Phillips *et al.*, 1996; Umebayashi *et al.*, 2008; Berdanier *et al.*, 2016). Partitioning the total axial xylem sap flux into the relative contributions of each growth ring is difficult because of the spatial resolution of standard sap flow sensors compared with the width of annual rings and uncertainty about which rings are being measured (Granier *et al.*, 1994; Phillips *et al.*, 1996; Bush *et al.*, 2010; Berdanier *et al.*, 2016). Studies have addressed this issue with sap flow sensors installed at different depths (Phillips *et al.*, 1996; Gebauer *et al.*, 2008; Bush *et al.*, 2010; Berdanier *et al.*, 2016), dye tracing (Ellmore and Ewers 1986; Umebayashi *et al.*, 2008, 2010) and hydraulics experiments (Melcher *et al.*, 2003; Nolf *et al.*, 2017), all suggesting that in some species xylem sap can flow across annual growth ring boundaries.

Recruiting previous growth rings for axial xylem sap transport via cross-ring connections would increase the total number of functional xylem conduits, thereby increasing both network redundancy (Loepfe *et al.*, 2007) and the 'return' on the initial investment in past xylem production. In all species, cross-ring connections between growth rings allow older xylem to serve as a large capacitive reservoir to buffer the xylem sap from reaching excessively negative water potentials (Tyree and Zimmermann, 2002; Borchert and Pockman, 2005; Fukuda *et al.*, 2015; Matheny *et al.*, 2015). Cross-ring connections could also expand the xylem vessel network and allow multiple growth rings to contribute to axial flow (Fig. 1A). However, because deciduous leaves are connected to the current-year xylem, the lowest-resistance pathway for axial xylem sap transport would usually be through the current annual ring. Therefore, the previous-year rings likely contribute to axial flow if there is high evaporative demand, if the current-year xylem becomes dysfunctional from embolism or damage (Fig. 1B), or if there are partial or 'missing' growth rings (Lorimer *et al.*, 1999). If the current-year xylem becomes dysfunctional, xylem sap would need to move radially from the previous rings into the current-year xylem before

© The Author(s) 2019. Published by Oxford University Press on behalf of the Annals of Botany Company.
All rights reserved. For permissions, please e-mail: journals.permissions@oup.com.

Downloaded from https://academic.oup.com/aob/advance-article-abstract/doi/10.1093/aob/mcz076/5537005 by Bates College user on 19 August 2019

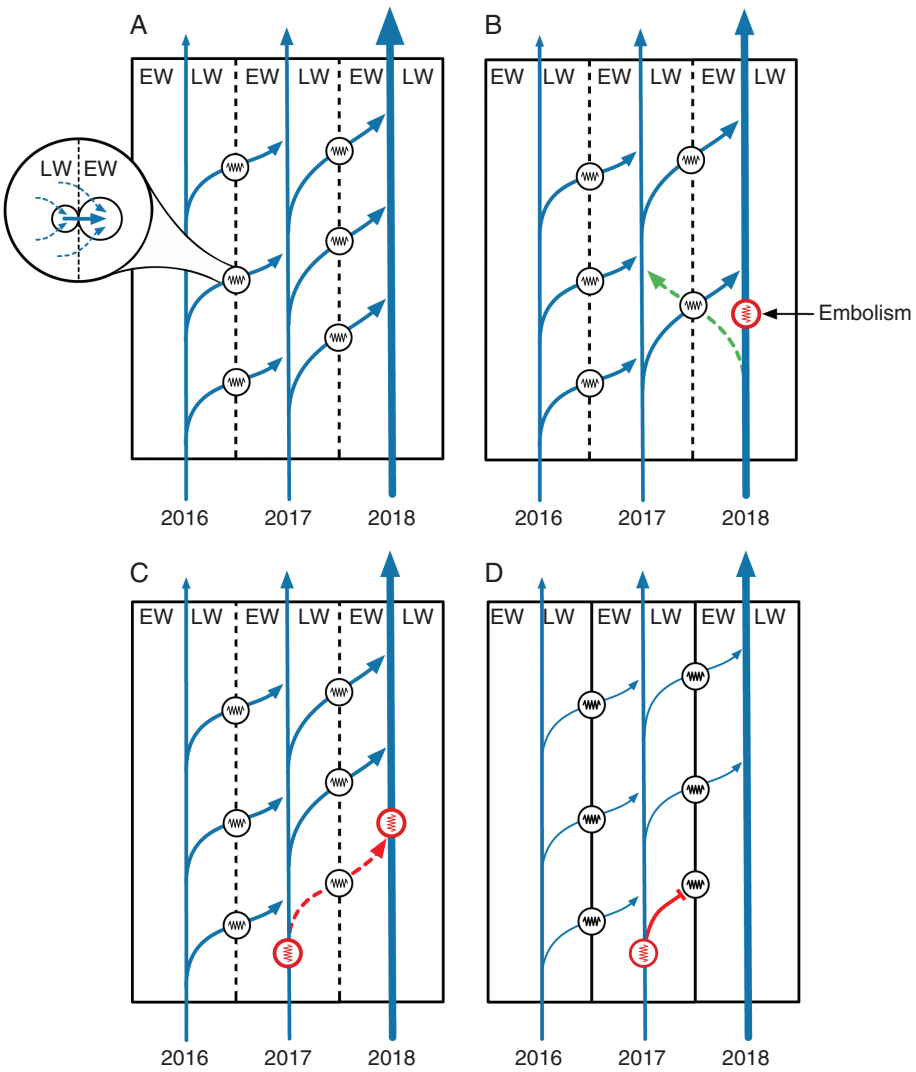

FIG. 1. Diagrammatic representation of some potential radial pathways for xylem sap and embolism movement between annual rings. In (A), the boundary between latewood (LW) and earlywood (EW) of subsequent years with inter-conduit connections (vertical dashed lines) allows significant contributions of previous growth rings to the axial bulk flow. Radial flow encounters resistance (horizontal resistor symbols), which can be divided into two categories [transverse view of two conduits shown in the inset in (A)]: low-resistance flow via pits (solid arrows) between xylem conduits (circles) and high-resistance flow through the cell walls (dashed arrow). In (B), an embolism (vertical resistor symbol) arising in the current-year ring (2018) blocks axial flow, but radial connectivity allows alternative pathways around the blockage but with increased resistance (dashed arrow in B). In (C), residual embolism in previous year xylem (2017) can follow the same radial inter-conduit pathways via pit membrane connections. In (D), species without direct connections via pits across the growth ring boundary (vertical solid lines) can isolate the spread of residual embolism to current-year xylem but the lack of cross-ring pitting results in very high resistance pathways for axial and radial contributions from older xylem [narrower curved arrows than in (A–C)].

it could enter the transpiration stream (Fig. 1B), either through lower-resistance direct intervessel connections or by diffusion through higher-resistance cell walls.

Embolism formation resulting from exposure to drought or freeze–thaw events (Sperry and Sullivan, 1992) can lead to hydraulic dysfunction. A larger interconnected multi-year xylem network would increase the number of alternative pathways for xylem sap transport (Ellmore *et al.*, 2006). However, an interconnected multi-year xylem network could also be a liability (Loepfe *et al.*, 2007), as residual emboli, unless blocked by tyloses or gums (Cochard and Tyree, 1990), could spread to the current-year xylem through the same cross-ring connections (Fig. 1C). Alternatively, the absence of cross-ring connections could isolate residual embolisms to previous growth rings (Choat *et al.*, 2015), thereby protecting the current-year growth from the legacy effects of past drought or frost (Fig. 1D). It is therefore important to determine the extent of cross-ring connections among species and their potential impact on xylem network organization and sap transport (Umebayashi *et al.*, 2008).

Identifying the specific pathway through which xylem sap travels across the latewood–earlywood boundary between two adjacent annual rings is critical for determining the resistance to radial xylem sap movement. Efficient radial flow of xylem sap across growth ring boundaries likely occurs through low-resistance pit membrane connections within pit fields between

Downloaded from https://academic.oup.com/aob/advance-article-abstract/doi/10.1093/aob/mcz076/5537005 by Bates College user on 19 August 2019

neighbouring cells (Tyree and Zimmermann, 2002). To our knowledge, direct cross-ring connections via inter-conduit pit fields have been identified and characterized in four species [*Fraxinus excelsior* (Oleaceae) (Burggraaf, 1972), *Machilus thunbergii* (Lauraceae) (Fujii *et al.*, 2001), *Fraxinus lanuginosa* (Oleaceae) (Kitin *et al.*, 2004) and *Cryptomeria japonica* (Cupressaceae) (Kitin *et al.*, 2009)]. The functional implications of such connections and their prevalence among other woody angiosperms therefore represent a major gap in our knowledge about the relationships between the structure and function of the xylem.

Isolating previous growth rings that contain embolisms could also be accomplished by limiting connections between earlywood and latewood within an annual ring rather than across growth ring boundaries (Burggraaf, 1972; Kitin *et al.*, 2004). In this case, cross-ring connections might allow embolism-resistant latewood to hydrate the cambium and developing earlywood vessels of the subsequent year (Kitin and Funada, 2016). However, the higher resistance of the smaller-diameter latewood vessels should contribute little to the overall conductivity once the earlywood of the subsequent year is fully developed. Particularly in ring-porous species, with large-diameter earlywood vessels that are likely to have earlywood vessels in previous growth rings embolized by freeze–thaw cycles (Davis *et al.*, 1999; Utsumi *et al.*, 1999), infrequent connections between the earlywood and latewood within an annual growth ring would limit the risk of embolism propagation to the latewood and subsequent year's earlywood.

Cross-ring connections, and the multi-year functionality of previous growth rings, may also impact measurements of stem vulnerability to embolism spread (Fukuda *et al.*, 2015; Nolf *et al.*, 2017). Including previous growth rings during hydraulics measurements of deciduous species may impact conductivity measurements by including vessels that are not connected to the transpiration stream and are non-functional *in planta*. For example, if previous growth rings are embolized (as in many ring-porous species after a freeze–thaw cycle; Davis *et al.*, 1999), maximum hydraulic conductivity measurements would be inflated following the standard technique of flushing embolisms. In contrast, in species that contain cross-ring connections it may be important to include the impact of previous growth rings that are still functional on measurements of whole-stem conductivity and resistance to embolism spread (Melcher *et al.*, 2003). It is therefore important to report the number of growth rings included in stem samples and consider other techniques, such as dye or tracer perfusion, to identify functional conduits during hydraulics measurements (Pratt *et al.*, 2018).

We searched for cross-ring connections in four northern hardwood species: *Acer rubrum*, *Fagus grandifolia*, *Fraxinus americana* and *Quercus rubra*. To locate and visualize cross-ring connections, we used dye staining and X-ray microcomputed tomography (microCT) imaging, a technique useful for visualizing complex structures in the xylem (Wason *et al.*, 2017). Finally, to determine how cross-ring connections and existing embolism in previous growth rings may impact vulnerability to embolism spread during drought in each species, we performed measurements to compare xylem vulnerability curves for branches containing only the current-year shoot with branches containing several years of growth.

MATERIALS AND METHODS

Vessel staining

To quantify and characterize cross-ring connections we tested whether dye injected into current-year shoot xylem could pass into previous growth rings. In our first experiment (Supplementary Data Fig. S1), we collected three or four stems per species ~50–70 cm long and containing 2–7 years of growth, on the proximal end of the stem from saplings of two diffuse-porous species (*Acer rubrum*, *Fagus grandifolia*) and two ring-porous species (*Fraxinus americana*, *Quercus rubra*) at Harvard Forest in Petersham, MA, USA, during August and September 2017. Current-year xylem was exposed by removing 75 % of the length of the current year's shoot from the distal end of the stem (Supplementary Data Fig. S1). The proximal and distal ends of the stem were both trimmed with a razor blade and fitted with tubing filled with deionized and 0.22-µm filtered water (Millipore Millipak, MilliporeSigma, USA). Native embolisms were removed by flushing stems (Sperry *et al.*, 1988) at 100 kPa from the proximal end containing multiple growth rings for 30–60 min. Following removal of native embolisms, stems were perfused with ~1 % safranin dye solution (using deionized and filtered water, as above) at 100 kPa from the current year's shoot until dye was visible in the solution exiting the multi-year end for 15 min (Supplementary Data Fig. S1). Perfusion of dye typically took 1–2 h. To minimize dye diffusion before the stems were sectioned, each sample was again flushed with water from the multi-year end and dye-stained stems were stored for 10 d at −80 °C before being sectioned.

In the first experiment (Supplementary Data Fig. S1B–D), some cross-ring connections may have been missed because most dye travelled through the low-resistance flow path in the current-year ring rather than crossing growth ring boundaries into previous growth rings (Fig. 1A). Therefore, we verified the results of our first experiment with a related experiment (Supplementary Data Fig. S1E–G) with two stems from each species that would block flow through the current-year ring (as in Fig. 1B). Branches were collected that contained 2 years of growth on the multi-year end and both ends were trimmed, as above. The current-year ring on the multi-year end was sealed with glue (Loctite 409, Loctite, Düsseldorf, Germany) before stems were rehydrated overnight using vacuum infiltration. The experiment then proceeded like the previous dye experiment, by injecting dye from the current-year end at 100 kPa for 45 min followed by flushing with water for 45 min from the multi-year end. Sealing the current-year (outer) ring on the multi-year end and only injecting dye from the current-year end would therefore force dye across growth rings if cross-ring connections were present. If no cross-ring connections were present, almost no dye should flow through the stem. In both experiments, a sliding microtome (Gärtner *et al.*, 2014) was used to collect cross-sections (7–9 µm thick) of each stem sample at ~1 cm below the dye insertion point in the current-year's growth and at the midpoint of each of the previous years' growth. Safranin is not soluble in Cytoseal 60 (Richard-Allan Scientific, MI, USA). Therefore, to avoid dye diffusion after sample preparation (Sano *et al.*, 2005), each cross-section was dehydrated in ethanol and mounted in Cytoseal 60. Sections were viewed on an Olympus BX60 compound microscope (Olympus Optical,

Downloaded from https://academic.oup.com/aob/advance-article-abstract/doi/10.1093/aob/mcz076/5537005 by Bates College user on 19 August 2019

Tokyo, Japan). Each cross-section was analysed visually to determine which growth rings contained dye-stained vessels and representative images were taken for each species (Canon EOS 6D, Canon, USA).

MicroCT imaging of cross-ring connections

We used high-resolution microCT, which allows non-destructive 3D imaging of tissues that can be viewed in any orientation, to identify anatomical features of potential cross-ring connections (Brodersen, 2013; Wason *et al.*, 2017). Although pit connections across growth rings may be visible in individual cross-sections using light microscopy, microCT allows detailed visualization of the extent of connections and examination of the 3-D nature of the cells involved. Xylem samples containing multiple growth rings were obtained by collecting one tree core (4.3 mm diameter) extracted at breast height with an increment borer from each of two canopy trees of *A. rubrum*, *Fagus grandifolia*, *Fraxinus americana* and *Q. rubra* at Harvard Forest. Tree cores were air-dried and dissected with a razor blade to a diameter of ~2.5 mm. Prepared tree core samples were transported to Beamline 8.3.2 at the Lawrence Berkeley National Laboratory Advanced Light Source, Berkeley, CA, USA, for imaging. The outer ~5 mm length of each core was imaged with two or three scans at different positions and 3-D reconstructions were completed following Wason *et al.* (2017). Final data sets were 3.2 × 3.2 × 2.7 mm with a voxel size of 1.25 μm^3. For each species, four to 12 growth rings were captured at this resolution.

MicroCT images were also collected at higher magnification, but with a smaller field of view, for more detailed investigations of the anatomy of growth ring boundaries and potential cross-ring connections. A transverse surface of a ~5-cm segment of the remaining sapwood from tree core samples was shaved flat with a microtome and examined under a dissecting microscope. For *A. rubrum*, three potential intervessel cross-ring connections were identified at low magnification with the dissecting microscope, marked, and trimmed to blocks of about 1.5 × 1.5 × 3 mm. For the remaining three species, ~10–15 growth ring boundaries were searched but no clear pairs of vessels with potential intervessel cross-ring connections were observed using the dissecting microscope. Therefore, for these three species one section of wood per species, containing two vessels near to each other across growth ring boundaries, was trimmed for scanning at high resolution. Each putative cross-ring connection was scanned at ×10 magnification yielding 3-D datasets that were 1.6 × 1.6 × 1.35 mm with a voxel size of 0.625 μm^3. These higher-resolution scans served to validate the presence of cross-ring connections observed in the broader search at lower resolution across multiple rings and to provide higher detail of the xylem anatomy of connections. Each microCT dataset was examined for cross-ring connections in Avizo 9.4 software (FEI, Hillsboro, OR, USA) using a combination of 2-D and 3-D visualizations to better understand the nature of cross-ring connections.

Xylem vulnerability curves

Cross-ring connections and inclusion of multiple growth rings may impact estimates of xylem resistance to embolism spread. Therefore, we constructed percentage loss of conductivity (PLC) curves using the benchtop dry-down method (Choat *et al.*, 2010). For each species, one curve was created using only the current-year shoot from branches (data presented in Wason *et al.*, 2018) and a second curve was created using segments that contained more than one growth ring on both ends of the segment (5.1 ± 2.8 years; grand mean ± s.d.; n = 10–15 per curve; sample details in Supplementary Data Table S1). Branches used for the benchtop dry-down curves were 1–2 m long and were collected predawn in late August and September of 2017 at Harvard Forest. The benchtop dry-down method and a modified Sperry apparatus (Sperry *et al.*, 1988) equipped with a flow meter (SLI-0430; Sensirion, Stäfa, Switzerland) was used to determine native conductivity (K_{nat}) and then maximum conductivity (K_{max}) after vacuum infiltration (full details are in Wason *et al.*, 2018). The resistance of the flow meter (inner diameter = 430 μm) was small compared with stem resistance (mean 0.26 % of stem resistance) and was removed during calculations. Final stem samples used for conductivity measurements were 10 ± 3.9 cm long (grand mean ± s.d.; sample details in Supplementary Data Table S1). We calculated PLC as $[1 - (K_{nat}/K_{max})] \times 100$. The PLC curves were fitted for each species and stem segment type (current-year or multi-year) using the Weibull or sigmoidal curves in the fitplc package in R (Duursma and Choat, 2017). In addition, xylem-area-specific native conductivities were calculated for each species using only current-year xylem area or total xylem area based on that species' ability to use previous-year growth rings, as indicated by microCT and dye-staining experiments, described above.

In addition to the benchtop dry-down curves, described above, in late September and early October 2016 we also used the centrifuge method (Alder *et al.*, 1997) to measure vulnerability curves for *A. rubrum*, *Fagus grandifolia* and *Fraxinus americana* (n = 5–6 branches per species). The centrifuge method requires 14-cm-long samples, which are not commonly available with current-year shoots for these species; therefore, centrifuge curves were measured on multi-year stems only. Briefly, multi-year stem segments (5.6 ± 3.8 years old; mean ± s.d.) were vacuum-infiltrated overnight to remove embolisms and K_{max} was measured, as described above and in Wason *et al.* (2018). Next, stems were mounted in a custom centrifuge chamber with reservoirs and sponges on the side walls to prevent exposure to air (Tobin *et al.*, 2013), and stems were spun to a desired water potential. Conductivity was measured on the Sperry apparatus (as described above) and stems were re-spun to successively more negative water potentials. This process was repeated until stems reached 100 % loss of conductivity (−4 MPa). Significant differences between vulnerability curves were determined using bootstrapped 95 % confidence intervals in the fitplc package in R (Duursma and Choat, 2017).

RESULTS

Dye movement across growth ring boundaries

All *A. rubrum* stems had xylem vessel staining that indicated cross-ring connections where dye moved from the current-year xylem to previous growth rings (Fig. 2A). In some samples of *A. rubrum*, previous growth rings were almost completely

Downloaded from https://academic.oup.com/aob/advance-article-abstract/doi/10.1093/aob/mcz076/5537005 by Bates College user on 19 August 2019

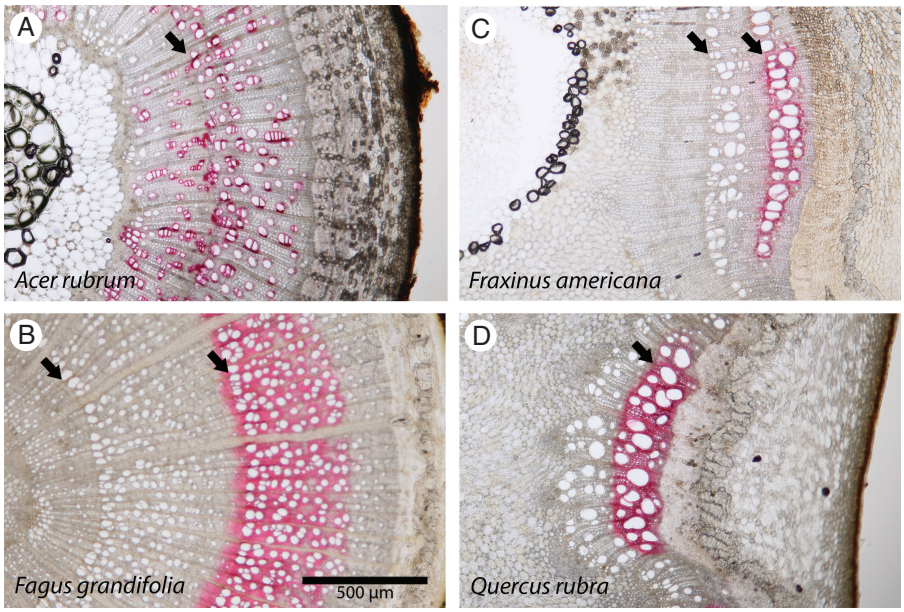

FIG. 2. Representative cross-sections of dye staining in 2- to 3-year-old stem sections. Stems were perfused with stain solution basipetally from the current-year shoot to determine whether the dye could reach previous growth rings. In each image, the pith and previous growth rings are to the left and the newer rings and epidermis are to the right. Arrows indicate growth ring boundaries. All vessels near the dye injection point in the current-year shoot were stained, and flow appeared to preferentially move through the largest-diameter vessels.

stained and in others only some of the latewood vessels that were nearest to the growth ring boundary were stained. The other diffuse-porous species, *Fagus grandifolia*, had dye-stained vessels primarily in the earlywood of the current-year growth ring (Fig. 2B). However, some dye did move across the growth ring boundary, but this dye movement was diffuse and not obviously associated with any vessels (Fig. 2B). The two ring-porous species, *Fraxinus americana* and *Q. rubra*, had dye-stained earlywood and latewood vessels only within the current year's growth ring (Fig. 2C, D). The second experiment (Supplementary Data Fig. S1), where the current-year growth ring was sealed on the multi-year end and dye was injected from the current year's shoot, confirmed these results. In *A. rubrum*, dye moved across the growth ring boundary, and in the remaining three species dye moved very short distances and only in the current-year ring.

Anatomical observations of cross-ring connections

MicroCT image analysis of growth ring boundaries supported the dye-staining results. In *A. rubrum*, 18 cross-ring connections were detected in a total of 13 analysed growth rings (Table 1) in both the higher (0.625 μm^3)- and lower (1.25 μm^3)-resolution scans. Cross-ring connections in *A. rubrum* had latewood vessels in the previous-year xylem that were 2.5 times smaller in diameter than the earlywood vessels to which they connect (Table 1, Fig. 3A, B). However, cross-ring connections in *A. rubrum* were not directly between two vessels, but instead formed by an imperforate tracheary element between the two vessels at the growth ring boundary. These tracheary elements had extensive pit fields (arrow in Fig. 3C) in both periclinal walls, thereby forming a vessel–'imperforate tracheary element'–vessel connection spanning the growth ring boundary (Figs 3D–F and 4). In *Fraxinus americana*, 12 cross-ring intervessel connections were detected in eight growth rings analysed with microCT (Table 1). Intervessel cross-ring connections in *Fraxinus americana* had latewood vessels with a diameter 10 times smaller than the earlywood vessels they connected to across the growth ring boundary (Table 1; Fig. 5A, B) with dense intervessel pitting (Fig. 5C–F). No cross-ring connections were observed in microCT images of *Fagus grandifolia* (Supplementary Data Fig. S2) or *Q. rubra* (Table 1). No species had direct cross-ring connections between fibres or tracheids.

Xylem vulnerability curves

We compared PLC curves generated for each species using two different methods. First, the benchtop method was used for current-year stems (reported in Wason *et al.*, 2018) because of the limitations of minimum sample length required for the centrifuge. We then compared these data with benchtop-derived curves for multi-year stems as well as centrifuge PLC curves for multi-year stems. For both *A. rubrum* and *F. grandifolia*, benchtop and centrifuge curves generally showed good agreement. Current-year *A. rubrum* stems had a more negative water potential at 12 % loss of conductivity (P_{12}) than multi-year stems from the centrifuge method, and less negative P_{88} than multi-year stems from the benchtop method, but otherwise the three curves were not significantly different based on overlapping 95 % confidence intervals (Fig. 6A; Table 2). Current-year *Fagus grandifolia* stems had similar resistance to embolism spread as multi-year stems using the benchtop method (Fig. 6B, Table 2); however, P_{50} for multi-year stems from the centrifuge method was 1 MPa more negative than from the benchtop method (Fig. 6B, Table 2).

Downloaded from https://academic.oup.com/aob/advance-article-abstract/doi/10.1093/aob/mcz076/5537005 by Bates College user on 19 August 2019

TABLE 1. *Frequency of cross-ring intervessel connections in xylem of four northern hardwood trees from the north-eastern USA observed using X-ray microCT. Total tangential area searched was the total area of all growth rings that were examined via microCT. Mean earlywood and latewood diameters are reported for vessels connected across growth rings*

Species	Cross-ring intervessel connections	Number of rings searched	Total tangential area searched (mm^2)	Earlywood vessel diameter, µm (mean ± s.d.)	Latewood vessel diameter µm (mean ± s.d.)
Acer rubrum	18	13	40.8	52.8 ± 17.1	21.1 ± 6.7
Fagus grandifolia	0	5	25.2	–	–
Fraxinus americana	12	8	32.0	227 ± 22.8	21.3 ± 4.9
Quercus rubra	0	7	29.8	–	–

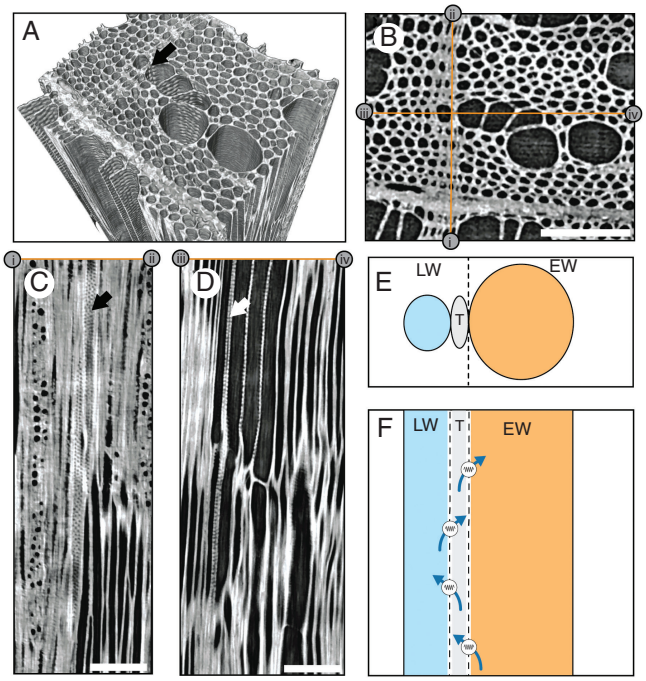

FIG. 3. MicroCT scans (0.625 μm^3 resolution) of xylem in *Acer rubrum* showing a cross-ring connection between vessels. (A) Volume rendering of a 0.25 × 0.3 × 0.75-mm block of xylem tissue showing a cross-ring connection (arrow) between the latewood (left) and earlywood vessel (right). The earlywood vessel also connects to a radial file of other earlywood vessels with extensive pitting. (B) Transverse slice from the top of the block showing vessel lumen in black and xylem tissue in white. The locations of the (C) tangential (i, ii) and (D) radial (iii, iv) slices are indicated in (B). (C) Tangential slice approximately parallel to the growth ring boundary showing the pitted vessel wall (arrow) at the growth ring boundary. (D) Radial view showing the extensive pitting on both walls of the imperforate tracheary element between the latewood (left) and earlywood (right) vessel (arrow). (E) Diagram of transverse view (as in B) showing connections across the growth ring boundary (dashed line) between large-diameter earlywood (EW) and narrow-diameter latewood (LW) vessels separated by an imperforate tracheary element (T). (F) Radial view (as in D) depicting potential cross-ring flow (arrows) between latewood (LW) and earlywood (EW) vessels through the tracheary element (T). Scale bars (B–D) = 100 µm. Scale bar in (B) can be used as a reference for the 3-D rendering in (A).

In the long-vesselled species *Q. rubra* and *F. Americana*, multi-year PLC curves did not match current-year PLC curves. For both species, the centrifuge method suggested that stems were highly vulnerable compared with the current-year benchtop curves. Current-year *Fraxinus americana* stems were more resistant to embolism spread than the apparently very vulnerable multi-year stems, but all three curves converged at >90 % loss of conductivity at water potentials below −1.8 MPa (Fig. 6C, Table 2). Current-year *Q. rubra* stems were more resistant to embolism spread than the apparently very vulnerable multi-year stems at water potentials down to −2.5 MPa (Fig. 6D, Table 2).

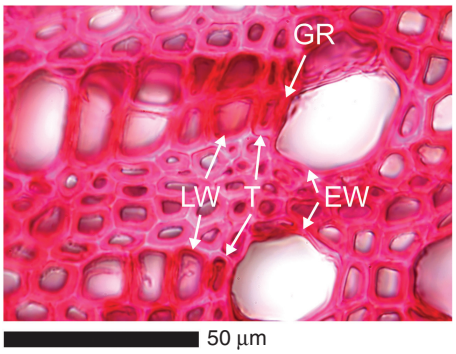

FIG. 4. Example of connections across a growth ring boundary (GR) in *Acer rubrum* showing imperforate tracheary elements (T) between the latewood (LW) and earlywood (EW) vessels in a transverse section stained with safranin.

Dye-staining and microCT data suggest that *A. rubrum* can use more than one growth ring for axial transport, whereas *Fagus grandifolia*, *Fraxinus americana* and *Q. rubra* use only the current-year growth ring. Therefore, we standardized native conductivity by the xylem area used for axial transport in each species. Generally, xylem-specific conductivity of multi-year stems aligned with current-year stems (Fig. 7A–D) except for *Fagus grandifolia* and *Q. rubra*, where conductivities were slightly higher than expected from current-year stems (Fig. 7B, D).

DISCUSSION

Presence of cross-ring connections

Cross-ring connections observed in *A. rubrum* with dye staining and microCT are consistent with dye-staining, sap flow and hydraulics experiments on other *Acer* spp. (Braun, 1970; Chaney and Kozlowski, 1977; Melcher *et al.*, 2003; Umebayashi *et al.*, 2008) and other diffuse-porous species (Umebayashi *et al.*, 2008; Berdanier *et al.*, 2016). Rather than direct intervessel connections, as observed in the only other diffuse-porous species studied in this detail [*Machilus thunbergii* (Lauraceae); Fujii *et al.*, 2001], cross-ring connections in *A. rubrum* were characterized by imperforate tracheary elements at the growth ring boundary with extensive pitting on both periclinal walls (Figs 3 and 4). Latewood vessels were narrower than earlywood vessels across the growth ring boundary and dye did not stain every vessel in previous growth rings, suggesting that cross-ring sap flow has a higher resistance than axial sap flow. This

Downloaded from https://academic.oup.com/aob/advance-article-abstract/doi/10.1093/aob/mcz076/5537005 by Bates College user on 19 August 2019

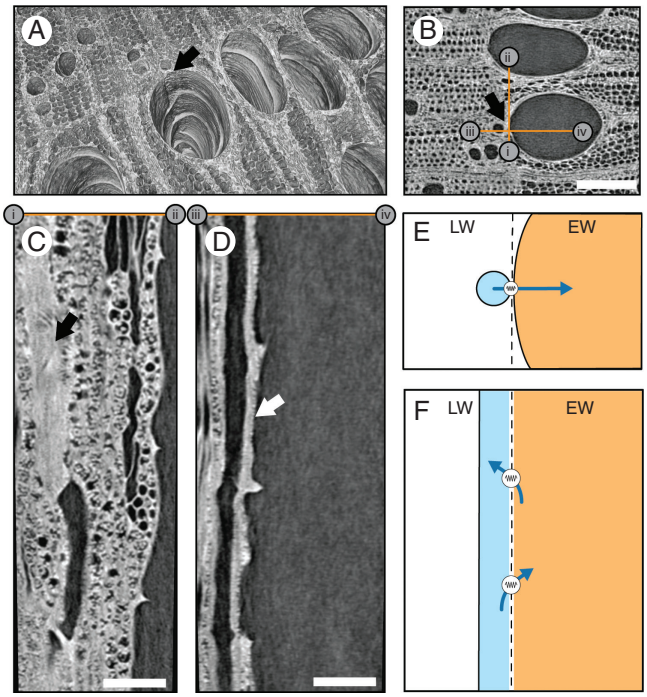

FIG. 5. MicroCT scans (1.25 μm³ resolution) of xylem in *Fraxinus americana* showing a cross-ring connection between vessels. (A) Overhead and slightly angled view of a volume rendering of the tangential surface of the xylem tissue visible in (B). (B) Transverse slice through the xylem showing vessel lumen in black and xylem tissue in white and the cross-ring connection (arrow) between the latewood (left) and earlywood vessel (right). Note the rough-textured cell wall between the two vessels indicating cross-ring pitting [arrow in (A)]. The locations of the (C) tangential (i, ii) and (D) radial (iii, iv) slices are indicated in (B). (C) Tangential slice parallel to the growth ring boundary showing the pitted vessel wall (arrow) between the latewood and earlywood vessels. (D) Radial view showing the pitting between the latewood and earlywood vessel (arrow). (E) Diagram of transverse view (as in B) showing connections across the growth ring boundary (dashed line) between large-diameter earlywood (EW) and narrow-diameter latewood (LW) vessels. (F) Radial view (as in D) depicting potential cross-ring flow (arrows) between latewood (LW) and earlywood (EW) vessels. Scale bar (B) = 200 μm; (C, D) = 100 μm. Scale bar in (B) can be used as a reference for the 3-D rendering in (A). Note that this scan was collected at lower resolution, and therefore has less detail, than the scan in Fig. 3.

finding supports previous data showing that 30–50 % of the axial flow in *Acer* sp. occurs in previous growth rings (Melcher *et al.*, 2003; Spicer and Holbrook, 2005).

We found no evidence of cross-ring connections in the other diffuse-porous species, *Fagus grandifolia*. The growth ring boundary was composed of parenchyma cells and narrow fibres with sporadic pitting on radial (anticlinal) walls only. We also found little to no staining in the latewood of the current-year ring, similar to *Fagus japonica* (Umebayashi *et al.*, 2008), suggesting that *Fagus* spp. latewood may be a high-resistance pathway with a limited role in axial sap transport. The lack of cross-ring connections but apparent diffusion across the growth ring boundary suggests that previous growth rings may be accessible via higher-resistance pathways, such as flow through cell walls or extracellular spaces.

Although most deciduous ring-porous species primarily use current-year growth rings for axial xylem sap transport (Chaney and Kozlowski, 1977; Ellmore and Ewers, 1986; Berdanier *et al.*, 2016), connections have been observed in *Fraxinus* species (Braun, 1970; Burggraaf, 1972; Kitin *et al.*, 2004). We found 12 cross-ring intervessel connections in the ring-porous species *Fraxinus americana* (Fig. 5), as observed in the similar species, *Fraxinus lanuginosa* (Kitin *et al.*, 2004). Despite these connections, dye did not flow across growth ring boundaries (Fig. 2C), as also found by Chaney and Kozlowski (1977), likely because the much higher resistance in narrow latewood vessels (and occasional latewood vascular tracheids) compared with the wide earlywood vessels to which they connect. Therefore, latewood conduits in previous rings of *Fraxinus* spp. are unlikely to serve as a redundant axial flow pathway, but instead may keep the cambium and developing leaves hydrated during earlywood development (Kudo *et al.*, 2015; Kitin and Funada, 2016).

In the other ring-porous species, *Q. rubra*, we found no latewood vessels that paralleled earlywood vessels across a growth ring boundary and no evidence of any cross-ring connections. Although other *Quercus* spp. may have cross-ring connections via vasicentric tracheids (Sano *et al.*, 2011), we found no evidence of dye stain crossing growth ring boundaries in *Q. rubra*. This suggests that *Q. rubra* may rely almost completely on the current-year ring for axial transport. Our results support previous findings (Spicer and Holbrook, 2005; Umebayashi *et al.*, 2008), indicating that in temperate deciduous ring-porous species such as *Q. rubra* most sap flow occurs in outermost regions of the sapwood.

Significance of cross-ring connections

Cross-ring connections in *A. rubrum* and other *Acer* spp., as well as the ability to use previous growth rings for xylem sap transport, may explain missing growth rings in *Acer* spp. (Lorimer *et al.*, 1999) and why *Acer* spp. show evidence of vulnerability segmentation (Choat *et al.*, 2005; Lens *et al.*, 2011; Brodersen, 2016; Gleason *et al.*, 2016; Wason *et al.*, 2018). *Acer rubrum* has more resistant pit membranes in multi-year branches than the other four species (Wason *et al.*, 2018), perhaps to limit embolism spread in xylem that will be used for multiple years. For *A. rubrum*, vulnerability curves were nearly identical for stems with current-year xylem only and stems with multiple rings (Figs 6 and 7). This contrasts with studies suggesting that resistance to air seeding declined in older growth rings (Melcher *et al.*, 2003) or in the innermost ring containing primary xylem (Fukuda *et al.*, 2015), but supports other research showing no decline in resistance to air seeding for *A. rubrum* across three growth rings (Wason *et al.*, 2018).

As in *A. rubrum*, most vessels in *Fagus grandifolia* are below the 44-μm diameter threshold (Wason *et al.*, 2018) above which embolism induced by freeze–thaw events can be problematic (Davis *et al.*, 1999). Therefore, previous growth rings in these diffuse-porous species may stay hydrated for many years, as found for the related species *Acer palmatum* and *Fagus japonica* (Umebayashi *et al.*, 2008). Hydrated previous growth rings in *Fagus grandifolia* may serve as a capacitor and buffer the effects of drought. Despite the lack of cross-ring connections in *Fagus grandifolia,* vulnerability curves of current-year and multi-year stems were similar, suggesting that the resistance to

Downloaded from https://academic.oup.com/aob/advance-article-abstract/doi/10.1093/aob/mcz076/5537005 by Bates College user on 19 August 2019

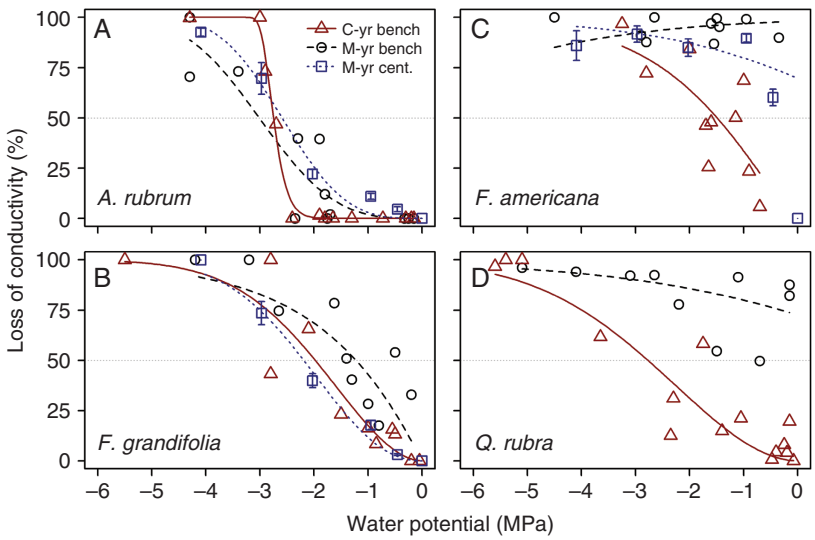

FIG. 6. Xylem vulnerability curves for current year's growth only (C-yr; as reported in Wason *et al.*, 2018) or stems containing multiple growth rings (M-yr). Curves were created using either the benchtop dry-down method (bench) or the centrifuge method (cent.). Centrifuge curves were generated from five or six stems per species and each point represents the mean ± one standard error. All curves are modelled with Weibull functions except the multi-year curves in (C) and (D), which would not converge and are therefore modelled with sigmoidal functions.

TABLE 2. *Water potentials (MPa) at 12 % (P_{12}), 50 % (P_{50}) and 88 % (P_{88}) loss of conductivity (PLC) for the four study species (with bootstrapped 95 % confidence intervals). Values are reported for benchtop curves conducted on current-year (C-yr) and multi-year (M-yr) stems as well as from centrifuge curves on multi-year stems. Estimates are not available (NA) when the mean lines or 95 % confidence intervals do not cross P_{12}, P_{50} or P_{88} within the sampled data range (see Table 2, Fig. 6). Water potentials within a row with overlapping confidence intervals share a letter*

Species	PLC	C-yr benchtop	M-yr benchtop	M-yr centrifuge
Acer rubrum	P_{88}	−2.9 (−3.0, −2.9)^{a}	−4.3 (NA – −3.1)^{b}	−3.6 (NA to −2.7)^{ab}
	P_{50}	−2.7 (−2.9, −2.7)^{a}	−3.0 (−3.8, −2.4)^{a}	−2.6 (−3.1, −2.3)^{a}
	P_{12}	−2.5 (−2.8, −2.3)^{a}	−1.8 (−3.1, −1.2)^{ab}	−1.6 (−2.1, −1.1)^{b}
Fagus grandifolia	P_{88}	−3.6 (NA, 2.4)^{a}	−3.6 (NA, −1.9)^{a}	−3.6 (NA, −2.8) ^{A}
	P_{50}	−2.0 (−3.3, −1.5)^{ab}	−1.2 (−1.6, −0.6)^{a}	−2.2 (−2.6, −1.8)^{b}
	P_{12}	−0.8 (−1.2, −0.5)^{a}	−0.2 (−0.8, NA)^{a}	−1.0 (−1.7, −0.7)^{a}
Fraxinus americana	P_{88}	−3.5 (NA, −2.2)	−4.0 (−2.4, NA)	−2.1 (NA, −0.6)
	P_{50}	−1.5 (−2.1, −0.9)	NA	NA
	P_{12}	−0.4 (−1.0, NA)	NA	NA
Quercus rubra	P_{88}	−5.0 (NA, −2.7)	−2.5 (NA, −0.9)	–
	P_{50}	−2.8 (−3.4, −1.7)	NA	–
	P_{12}	−1.1 (−2.2, −0.5)	NA	–

embolism spread in these rings had not declined. Furthermore, normalizing native conductivity by current-year xylem area overestimated xylem specific conductivity, suggesting that previous growth rings were still hydrated and transported water when exposed on both ends of the segment, although they would not directly connect to the transpiration stream *in planta*.

In *Fraxinus americana* and *Q. rubra*, earlywood vessels are large enough to experience freeze–thaw embolisms (Wason *et al.*, 2018), while most latewood vessels are not (Davis *et al.*, 1999; Umebayashi *et al.*, 2008). Furthermore, many earlywood vessels in previous-year growth rings of the ring-porous species *Q. rubra* and *F. americana* can be blocked by tyloses (Meyer and Côté, 1968; Cochard and Tyree, 1990; Micco *et al.*, 2016). Indeed, we found that normalizing native conductivity by current-year xylem area better estimated xylem-specific conductivity for *Fraxinus americana* (Fig. 7C). Normalizing conductivity of multi-year stems to current-year xylem area for *Q. rubra* led to slight overestimation of conductivity (Fig. 7D), perhaps related to vessel size or density differences between the current-year ring and previous growth rings that contain primary growth with fewer and smaller vessels per area (Fig. 2D; Wason *et al.*, 2018).

With residual embolisms in earlywood of previous growth rings, cross-ring connections could provide a pathway for embolisms to spread into current-year xylem. Despite having cross-ring intervessel connections, *Fraxinus* spp. have a reduced risk of embolism spread by limiting earlywood-to-latewood vessel connections within a ring (Burggraaf, 1972; Kitin *et al.*, 2004). Indeed, in one microCT sample we found that across four growth rings and 44 earlywood vessels, only two connected to latewood vessels within the same ring whereas four connected to latewood vessels across a ring boundary. In *Q. rubra*, on the other hand, the absence of any cross-ring connections further reduces the risk of residual embolism

Downloaded from https://academic.oup.com/aob/advance-article-abstract/doi/10.1093/aob/mcz076/5537005 by Bates College user on 19 August 2019

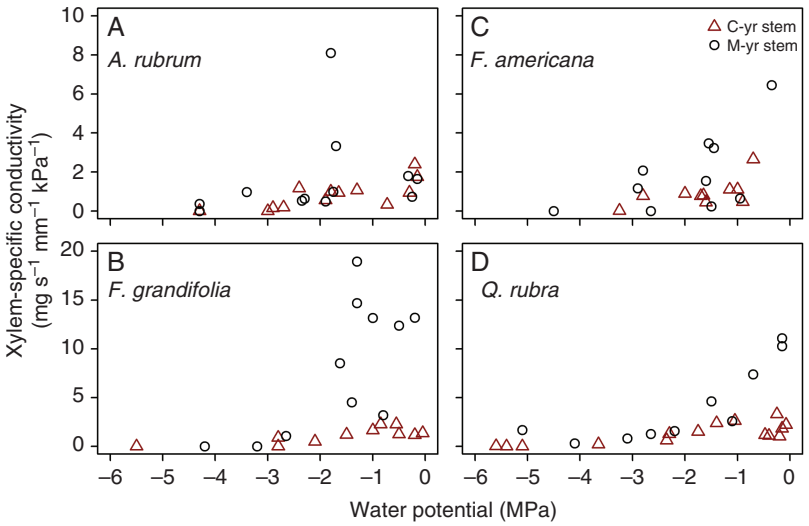

FIG. 7. Native xylem-specific conductivity of stems containing only current-year (C-yr) xylem or multiple years (M-yr) of xylem. Conductivities were normalized by the xylem area of functional growth rings based on dye staining and microCT analysis: total xylem cross-sectional area for (A) *Acer rubrum*, and current-year xylem cross-sectional area for (B) *Fagus grandifolia*, (C) *Fraxinus americana*, and (D) *Quercus rubra*. Note: *y*-axis scaling differs between top and bottom panels.

spreading into the current-year growth ring. Importantly, the lack of dye spreading into previous growth rings of *Fraxinus americana*, *Q. rubra* and *Fagus grandifolia* further supports the ephemeral nature of each growth ring for axial xylem sap transport and may explain the lack of vulnerability segmentation in these species (Wason *et al.*, 2018) and strong segmentation of *Acer* spp. (Choat *et al.*, 2005; Johnson *et al.*, 2016; Wason *et al.*, 2018).

SUPPLEMENTARY DATA

Supplementary data are available online at https://academic.oup.com/aob and consist of the following. Figure S1: schematic diagram of the two dye-staining experiments. Figure S2: microCT images of a growth ring boundary in *Fagus grandifolia*. Table S1: stem characteristics of samples used in hydraulics measurements.

FUNDING

This work was supported by the National Science Foundation (IOS-1557917). J.W.W. was partially supported by the USDA National Institute of Food and Agriculture, McIntire Stennis Project Number ME0-42001 through the Maine Agricultural and Forest Experiment Station.

ACKNOWLEDGEMENTS

We thank Harvard Forest and D. Parkinson for facilitating this research, as well as K. Anstreicher and A. Rubenstein for help with data collection. This research used resources of the Advanced Light Source, which is a DOE Office of Science User Facility under contract number DE-AC02-05CH11231.

LITERATURE CITED

Alder NN, Pockman WT, Sperry JS, Nuismer S. 1997. Use of centrifugal force in the study of xylem cavitation. *Journal of Experimental Botany* **48**: 665–674.

Berdanier AB, Miniat CF, Clark JS. 2016. Predictive models for radial sap flux variation in coniferous, diffuse-porous and ring-porous temperate trees. *Tree Physiology* **36**: 932–941.

Borchert R, Pockman WT. 2005. Water storage capacitance and xylem tension in isolated branches of temperate and tropical trees. *Tree Physiology* **25**: 457–466.

Braun HJ. 1970. *Funktionelle Histologie der sekundären Sprossachse*. Berlin: Gebrüder Borntraeger.

Brodersen CR. 2013. Visualizing wood anatomy in three dimensions with high-resolution X-ray micro-tomography (μCT) – a review. *IAWA Journal* **34**: 408–424.

Brodersen CR. 2016. Finding support for theoretical tradeoffs in xylem structure and function. *New Phytologist* **209**: 8–10.

Burggraaf PD. 1972. Some observations on the course of the vessels in the wood of *Fraxinus excelsior* L. *Acta Botanica Neerlandica* **21**: 32–47.

Bush SE, Hultine KR, Sperry JS, Ehleringer JR. 2010. Calibration of thermal dissipation sap flow probes for ring- and diffuse-porous trees. *Tree Physiology* **30**: 1545–1554.

Chaney WR, Kozlowski TT. 1977. Patterns of water movement in intact and excised stems of *Fraxinus americana* and *Acer saccharum* seedlings. *Annals of Botany* **41**: 1093–1100.

Choat B, Lahr EC, Melcher PJ, Zwieniecki MA, Holbrook NM. 2005. The spatial pattern of air seeding thresholds in mature sugar maple trees. *Plant, Cell & Environment* **28**: 1082–1089.

Choat B, Drayton WM, Brodersen C, *et al.* 2010. Measurement of vulnerability to water stress-induced cavitation in grapevine: a comparison of four techniques applied to a long-vesseled species. *Plant, Cell & Environment* **33**: 1502–1512.

Choat B, Brodersen CR, McElrone AJ. 2015. Synchrotron X-ray microtomography of xylem embolism in *Sequoia sempervirens* saplings during cycles of drought and recovery. *New Phytologist* **205**: 1095–1105.

Cochard H, Tyree MT. 1990. Xylem dysfunction in *Quercus*: vessel sizes, tyloses, cavitation and seasonal changes in embolism. *Tree Physiology* **6**: 393–407.

Davis SD, Sperry JS, Hacke UG. 1999. The relationship between xylem conduit diameter and cavitation caused by freezing. *American Journal of Botany* **86**: 1367–1372.

Duursma R, Choat B. 2017. fitplc – an R package to fit hydraulic vulnerability curves. *Journal of Plant Hydraulics* **4**: e-002.

Downloaded from https://academic.oup.com/aob/advance-article-abstract/doi/10.1093/aob/mcz076/5537005 by Bates College user on 19 August 2019

Ellmore GS, Ewers FW. 1986. Fluid flow in the outermost xylem increment of a ring-porous tree, *Ulmus americana*. *American Journal of Botany* **73**: 1771–1774.

Ellmore GS, Zanne AE, Orians CM. 2006. Comparative sectoriality in temperate hardwoods: hydraulics and xylem anatomy. *Botanical Journal of the Linnean Society* **150**: 61–71.

Fujii T, Lee S-J, Kuroda N, Suzuki Y. 2001. Conductive function of intervessel pits through a growth ring boundary of *Machilus thunbergii*. *IAWA Journal* **22**: 1–14.

Fukuda K, Kawaguchi D, Aihara T, *et al.* 2015. Vulnerability to cavitation differs between current-year and older xylem: non-destructive observation with a compact magnetic resonance imaging system of two deciduous diffuse-porous species. *Plant, Cell & Environment* **38**: 2508–2518.

Gärtner H, Lucchinetti S, Schweingruber FH. 2014. New perspectives for wood anatomical analysis in dendrosciences: the GSL1-microtome. *Dendrochronologia* **32**: 47–51.

Gebauer T, Horna V, Leuschner C. 2008. Variability in radial sap flux density patterns and sapwood area among seven co-occurring temperate broad-leaved tree species. *Tree Physiology* **28**: 1821–1830.

Gleason SM, Westoby M, Jansen S, *et al.* 2016. Weak tradeoff between xylem safety and xylem-specific hydraulic efficiency across the world's woody plant species. *New Phytologist* **209**: 123–136.

Granier A, Anfodillo T, Sabatti M, *et al.* 1994. Axial and radial water flow in the trunks of oak trees: a quantitative and qualitative analysis. *Tree Physiology* **14**: 1383–1396.

Johnson DM, Wortemann R, McCulloh KA, *et al.* 2016. A test of the hydraulic vulnerability segmentation hypothesis in angiosperm and conifer tree species. *Tree Physiology* **36**: 983–993.

Kitin P, Funada R. 2016. Earlywood vessels in ring-porous trees become functional for water transport after bud burst and before the maturation of the current-year leaves. *IAWA Journal* **37**: 315–331.

Kitin PB, Fujii T, Abe H, Funada R. 2004. Anatomy of the vessel network within and between tree rings of *Fraxinus lanuginosa* (Oleaceae). *American Journal of Botany* **91**: 779–788.

Kitin P, Fujii T, Abe H, Takata K. 2009. Anatomical features that facilitate radial flow across growth rings and from xylem to cambium in *Cryptomeria japonica*. *Annals of Botany* **103**: 1145–1157.

Kudo K, Yasue K, Hosoo Y, Funada R. 2015. Relationship between formation of earlywood vessels and leaf phenology in two ring-porous hardwoods, *Quercus serrata* and *Robinia pseudoacacia*, in early spring. *Journal of Wood Science* **61**: 455–464.

Lens F, Sperry JS, Christman MA, Choat B, Rabaey D, Jansen S. 2011. Testing hypotheses that link wood anatomy to cavitation resistance and hydraulic conductivity in the genus *Acer*. *New Phytologist* **190**: 709–723.

Loepfe L, Martinez-Vilalta J, Pinol J, Mencuccini M. 2007. The relevance of xylem network structure for plant hydraulic efficiency and safety. *Journal of Theoretical Biology* **247**: 788–803.

Lorimer CG, Dahir SE, Singer MT. 1999. Frequency of partial and missing rings in *Acer saccharum* in relation to canopy position and growth rate. *Plant Ecology* **143**: 189–202.

Matheny AM, Bohrer G, Garrity SR, Morin TH, Howard CJ, Vogel CS. 2015. Observations of stem water storage in trees of opposing hydraulic strategies. *Ecosphere* **6**: art165.

Melcher PJ, Zwieniecki MA, Holbrook NM. 2003. Vulnerability of xylem vessels to cavitation in sugar maple. Scaling from individual vessels to whole branches. *Plant Physiology* **131**: 1775–1780.

Meyer RW, Côté WA. 1968. Formation of the protective layer and its role in tylosis development. *Wood Science and Technology* **2**: 84–94.

Micco VD, Balzano A, Wheeler EA, Baas P. 2016. Tyloses and gums: a review of structure, function and occurrence of vessel occlusions. *IAWA Journal* **37**: 186–205.

Nolf M, Lopez R, Peters JMR, *et al.* 2017. Visualization of xylem embolism by X-ray microtomography: a direct test against hydraulic measurements. *New Phytologist* **214**: 890–898.

Phillips N, Oren R, Zimmermann R. 1996. Radial patterns of xylem sap flow in non-, diffuse- and ring-porous tree species. *Plant, Cell & Environment* **19**: 983–990.

Pratt RB, Jacobsen AL, Meinzer F. 2018. Identifying which conduits are moving water in woody plants: a new HRCT-based method. *Tree Physiology* **38**: 1200–1212.

Sano Y, Okamura Y, Utsumi Y. 2005. Visualizing water-conduction pathways of living trees: selection of dyes and tissue preparation methods. *Tree Physiology* **25**: 269–275.

Sano Y, Morris H, Shimada H, Ronse De Craene LP, Jansen S. 2011. Anatomical features associated with water transport in imperforate tracheary elements of vessel-bearing angiosperms. *Annals of Botany* **107**: 953–964.

Sperry JS, Sullivan JEM. 1992. Xylem embolism in response to freeze-thaw cycles and water stress in ring-porous, diffuse-porous, and conifer species. *Plant Physiology* **100**: 605–613.

Sperry JS, Donnelly JR, Tyree MT. 1988. A method for measuring hydraulic conductivity and embolism in xylem. *Plant, Cell & Environment* **11**: 35–40.

Spicer R, Holbrook NM. 2005. Within-stem oxygen concentration and sap flow in four temperate tree species: does long-lived xylem parenchyma experience hypoxia? *Plant, Cell & Environment* **28**: 192–201.

Tobin MF, Pratt RB, Jacobsen AL, De Guzman ME. 2013. Xylem vulnerability to cavitation can be accurately characterised in species with long vessels using a centrifuge method. *Plant Biology* **15**: 496–504.

Tyree MT, Zimmermann MH. 2002. *Xylem structure and the ascent of sap*. Berlin: Springer.

Umebayashi T, Utsumi Y, Koga S, *et al.* 2008. Conducting pathways in north temperate deciduous broadleaved trees. *IAWA Journal* **29**: 247–263.

Umebayashi T, Utsumi Y, Koga S, *et al.* 2010. Xylem water-conducting patterns of 34 broadleaved evergreen trees in southern Japan. *Trees* **24**: 571–583.

Utsumi Y, Sano Y, Funada R, Fujikawa S, Ohtani J. 1999. The progression of cavitation in earlywood vessels of *Fraxinus mandshurica* var *japonica* during freezing and thawing. *Plant Physiology* **121**: 897–904.

Wason JW, Huggett BA, Brodersen CR. 2017. MicroCT imaging as a tool to study vessel endings in situ. *American Journal of Botany* **104**: 1424–1430.

Wason JW, Anstreicher KS, Stephansky N, Huggett BA, Brodersen CR. 2018. Hydraulic safety margins and air-seeding thresholds in roots, trunks, branches and petioles of four northern hardwood trees. *New Phytologist* **219**: 77–88.

Downloaded from https://academic.oup.com/aob/advance-article-abstract/doi/10.1093/aob/mcz076/5537005 by Bates College user on 19 August 2019